Design and Optimization of a Class-E Amplifier for a Loosely Coupled Planar Wireless Power System

Joaquin J. Casanova, *Student Member, IEEE*, Zhen Ning Low, *Student Member, IEEE*, and Jenshan Lin, *Senior Member, IEEE*

***Abstract*—In wireless power systems for charging battery-operated devices, the selection of component values guaranteeing certain desired performance characteristics can be a tedious trial-and-error process, either sweeping component values in circuit simulations or changing components by hand. This difficulty is compounded by the variable nature of the load resistance presented by a device under charge. This brief considers component selection for a specific wireless power system architecture, which is an open-loop class-E inverter using a series–parallel arrangement for load impedance transformation. Formulas for the optimal receiver, transmitter, and class-E components are derived given a set of constraints on the resistance, phase, quality factor, and drain voltage waveform. Using a 16 cm × 18 cm primary and a 4 cm × 5 cm secondary coil, the derived formulas are used to build a wireless power system. We show that the system has desirable performance characteristics, including a power delivery of over 3.7 W, peak efficiency of over 66%, and decreasing power delivery with increasing load resistance.**

***Index Terms*—Class E, inductive coupling, wireless power transfer.**

I. Introduction

A wireless charging system for battery-operated consumer electronics equipped with receiving coils could cut the last wire of portable devices [1], [2]. Near-field inductive coupling has promise as a wireless power technology [3]–[6].

Fig. 1 shows a block diagram for a generalized wireless power system, and the circuit diagram is shown in Fig. 2. The inverter is a class-E amplifier [7] driven by a low-power clock at 240 kHz, followed by a series–parallel impedance transformation network [8]. Selecting the values of $C_{\rm rx}$, $L_{\rm out}$, $C_{\rm out}$, and C_t for optimum performance of the wireless power system presents a challenge. Reference [9] shows the design methodology for a similar architecture with closed-loop control, which allows control of power delivery under variable loading conditions. Reference [10] demonstrates how to choose design values for a class E without relying on Raab's waveform equations; however, it involves numerical root finding. Reference [11] presents a selection technique for an open-loop system that relies on numerically sweeping component values until the impedance and drain voltage satisfy certain constraints, and [12] demonstrates the same for a multiple transmitter/receiver system. While this method successfully finds appropriate component values, it is time consuming. This brief derives simple formulas for the optimum component values by applying the same constraints. This open-loop system has the advantage of power regulation under a variable load, without the added complexity and minimum battery supply voltage associated with a closed-loop system as in [9].

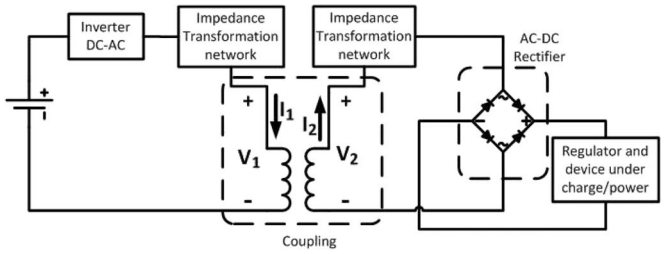

Fig. 1. One-to-one wireless power system block diagram.

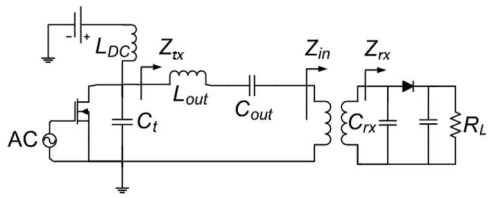

Fig. 2. Class-E driving circuit for a wireless power system.

II. Analysis

The optimum values for $C_{\rm rx}$, $L_{\rm out}$, $C_{\rm out}$, and C_t can be derived by applying several constraints on the system's response to the variable load resistance R_L. In this analysis, it is assumed that the components are lossless. In addition, assumptions are made about the class E to allow using Raab's equations [13], namely, that the transistor is a perfect switch and that the choke inductance is infinite. Before these derivations, it is necessary to have expressions for receiver impedance, i.e., $Z_{\rm rx}$, input impedance looking into the transmitter coil, i.e., $Z_{\rm in}$, and impedance looking into $L_{\rm out}$, i.e., $Z_{\rm tx}$. $Z_{\rm rx}$ can be expressed as follows:

$$Z_{\rm rx} = R_{\rm rx} + jX_{\rm rx} = R_L \| C_{\rm rx} \quad (1)$$

$$= \frac{R_L - j\omega C_{\rm rx} R_L^2}{1 + \omega^2 R_L^2 C_{\rm rx}^2}. \quad (2)$$

Manuscript received May 18, 2009; revised July 22, 2009 and August 13, 2009. First published October 30, 2009; current version published November 18, 2009. This work was supported by WiPower Inc. and Florida High Tech Corridor Council. This paper was recommended by Associate Editor D. Heo.

The authors are with the Department of Electrical and Computer Engineering, University of Florida, Gainesville, FL 32611 USA (e-mail: jcasa@ufl.edu; znlow@ufl.edu; jenshan@ufl.edu).

Color versions of one or more of the figures in this paper are available online at http://ieeexplore.ieee.org.

Digital Object Identifier 10.1109/TCSII.2009.2032465

$Z_{\rm in}$ can be found by examining the following coupling equations:

$$\begin{aligned} V_1 &= j\omega L_1 I_1 + j\omega M I_2 \\ V_2 &= j\omega M I_1 + j\omega L_2 I_2 \end{aligned} \tag{3}$$

where L_1, L_2, and M are the transmitter coil, receiver coil, and mutual inductance, respectively. $Z_{\rm in}$ is V_1/I_1, i.e.,

$$\begin{aligned} Z_{\rm in} &= R_{\rm in} + jX_{\rm in} \\ &= \frac{\omega^2 M^2 R_{\rm rx}}{R_{\rm rx}^2 + (\omega L_2 + X_{\rm rx})^2} \\ &\quad + j\left(\omega L_1 - \frac{\omega^2 M^2 (\omega L_2 + X_{\rm rx})}{R_{\rm rx}^2 + (\omega L_2 + X_{\rm rx})^2}\right). \end{aligned} \tag{4}$$

$Z_{\rm tx}$ is just $Z_{\rm in}$ with an additional series reactance from $C_{\rm out}$ and $L_{\rm out}$, i.e.,

$$\begin{aligned} Z_{\rm tx} &= R_{\rm tx} + jX_{\rm tx} \\ &= R_{\rm in} + j\left(\omega L_{\rm out} - \frac{1}{\omega C_{\rm out}} + X_{\rm in}\right). \end{aligned} \tag{5}$$

A. Design Equation for $C_{\rm rx}$

Selection of $C_{\rm rx}$ is determined on the basis of efficiency and quality factor Q of $Z_{\rm tx}$. If the real part of $Z_{\rm in}$ is too low compared with the coil parasitics, the system will be inefficient. If it is too large, it is difficult to get Q high enough for class-E operation (about 1.78 [14]). By forcing the peak real part of $Z_{\rm in}$ to be a specified value, i.e., R_0, a compromise between efficiency and Q can be reached. To derive which $C_{\rm rx}$ forces the maximum real part of $Z_{\rm in}$ to be R_0, the R_L corresponding to the peak value is found by setting $\partial R_{\rm in}/\partial R_L$ to zero. This yields a polynomial of degree six, where four of the roots are composed of a double conjugate pair and can thus be ignored. Thus

$$R_L = \pm\frac{j}{\omega C_{\rm rx}}. \tag{6}$$

There are two real roots, i.e.,

$$R_L = \pm\frac{\omega L_2}{1 - \omega^2 L_2 C_{\rm rx}} \tag{7}$$

which can be substituted back into (4); then, the real part is set to R_0, i.e.,

$$R_{\rm in} = \pm\frac{M}{2L_2}\frac{\omega M}{\omega^2 C_{\rm rx} L_2 - 1} = R_0. \tag{8}$$

Solving for $C_{\rm rx}$ yields two roots, i.e.,

$$C_{\rm rx} = \frac{R_0 L_2 \pm \frac{1}{2}\omega M^2}{R_0 \omega^2 L_2^2}. \tag{9}$$

The negative root gives a $C_{\rm rx}$ value that ensures that the $Z_{\rm in}$ phase will increase with increasing R_L, which has the desirable effect of lowering power delivery at a high load resistance. This is desirable because, in the case of a device being charged, a high load resistance (thousands of ohms) corresponds to a fully charged condition and, thus, a low power requirement.

B. Design Equation for $L_{\rm out}$

The purpose of $L_{\rm out}$ is to ensure the circuit has a minimum Q high enough for proper functioning of the class E. Q is smallest when the real part of $Z_{\rm in}$ is highest, at R_0. Since $L_{\rm out}$ contributes the largest part of the reactance of $Z_{\rm tx}$, i.e.,

$$Q \sim \frac{\omega L_{\rm out}}{R_0} \tag{10}$$

$L_{\rm out}$ is found to be

$$L_{\rm out} = \omega^{-1} Q R_0. \tag{11}$$

C. Design Equation for $C_{\rm out}$

$C_{\rm out}$ brings the range of the phase of $Z_{\rm tx}$ to a range that allows zero-voltage switching (ZVS) operation of the class E and maximum efficiency. From [15], this phase range is 40° to 70°. By setting the minimum phase to a specified value, i.e., ϕ, efficient operation can be achieved. The location of the minimum phase is where

$$\frac{\partial \angle(Z_{\rm tx})}{\partial R_L} = 0 \tag{12}$$

which yields a quadratic equation in R_L with the roots

$$\begin{aligned} R_L = \pm 2R_0 &\left(\frac{L_2}{M}\right)^2 \\ &\times \sqrt{\frac{\omega C_{\rm out}\left(\omega L_1(k^2-1) - R_0 Q\right) - 1}{\omega C_{\rm out}\left(\omega L_1(k^2-1) - R_0(Q+2)\right) - 1}} \end{aligned} \tag{13}$$

where $k = \sqrt{M^2/L_1 L_2}$. Substituting (13) into (5) and setting $\tan(\phi) = X_{\rm tx}/R_{\rm tx}$ and squaring to eliminate the radical in the numerator yields a quadratic equation in $C_{\rm out}$, with two real roots, i.e.,

$$\begin{aligned} C_{\rm out} = \omega^{-1} &\left\{\omega L_1(1-k^2) + R_0\left(Q + 1 \pm \sec(\phi)\right)\right\} \\ &\times \left\{R_0^2\left(Q^2 + 2Q - \tan(\phi)^2\right) + 2QR_0\omega L_1(1-k^2)\right. \\ &\left. + \omega^2 L_1^2 (1-k^2)^2 + 2\omega L_1 R_0 (1-k^2)\right\}^{-1}. \end{aligned} \tag{14}$$

The greater root, corresponding to the positive ϕ, yields

$$C_{\rm out} = \frac{\omega^{-1}}{\omega L_1(1-k^2) + R_0\left(Q + 1 - \sec(\phi)\right)} \tag{15}$$

after simplification.

D. Design Equation for C_t

Finally, C_t is selected to guarantee ZVS operation of the class E. From [13], this optimum value of C_t, given a load resistance R, is

$$C_t = \frac{2\omega^{-1}}{\left(1 + \frac{\pi^2}{4}\right)R}. \tag{16}$$

Since the load resistance in the wireless power system is variable, C_t is selected based on the maximum R, which, for

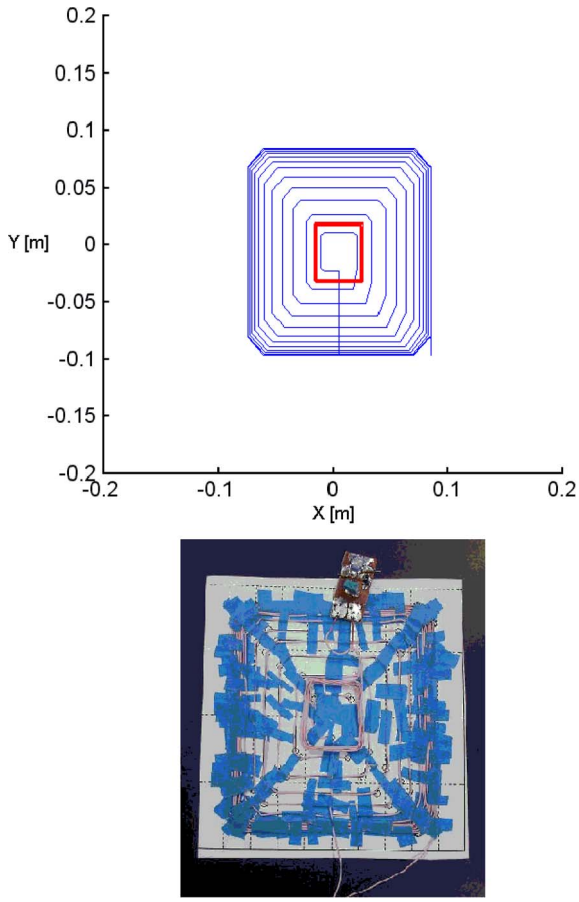

Fig. 3. Test setup. (Top) Coils, where red is the receiver and blue is the transmitter. (Bottom) Coils.

the circuit under consideration, is the magnitude of $Z_{\rm tx}$ as R_L increases to infinity. Taking this limit

$$R = \omega L_{\rm out} + \frac{1}{\omega C_{\rm out}} - \omega^2 M^2 \frac{\omega C_{\rm rx}}{\omega^2 C_{\rm rx} L_2 - 1} \tag{17}$$

and substituting in the derived values for the other components [see (9), (11), and (15)], the optimum C_t is found, i.e.,

$$C_t = \frac{2\omega^{-1}}{\left(1 + \frac{\pi^2}{4}\right)(1 + \sec(\phi))\, R_0}. \tag{18}$$

III. Experimental Results

Having derived the optimum component values for a given L_1, L_2, M, R_0, Q, and ϕ, this section demonstrates the performance of the system.

A test system was built, consisting of a 16 cm × 18 cm, 13-turn, spiral transmitting coil, which is designed by the technique described in [16], and a rectangular 4 cm × 5 cm, 6-turn, receiving coil. Both coils were constructed of 100-strand #40 American Wire Gauge Litz wires to minimize coil parasitics. The switching transistor was an IRLR3410, which was chosen because of its low output capacitance (typically below 100 pF), much lower than C_t. The IRLR3410 was driven with a gate voltage of 5 V and a supply voltage of 12 V, corresponding to a turn-on resistance of 0.125 Ω. Fig. 3 shows a picture

TABLE I
Design Parameters

Parameter	Value	Parasitic Resistance
L_1 (measured)	34.58 μH	0.39 Ω
L_2 (measured)	4.05 μH	0.09 Ω
M (measured)	1.65 μH	-
R_0	7.5 Ω	-
Q	2	-
ϕ	65^o	-

TABLE II
Component Values

Component	Calculated	Measured	Parasitic Resistance
C_{rx}	100.55 nF	100.00 nF	0.04 Ω
C_{out}	11.90 nF	11.57 nF	0.03 Ω
C_t	15.15 nF	14.55 nF	0.03 Ω
L_{out}	9.95 μH	9.52 μH	0.16 Ω

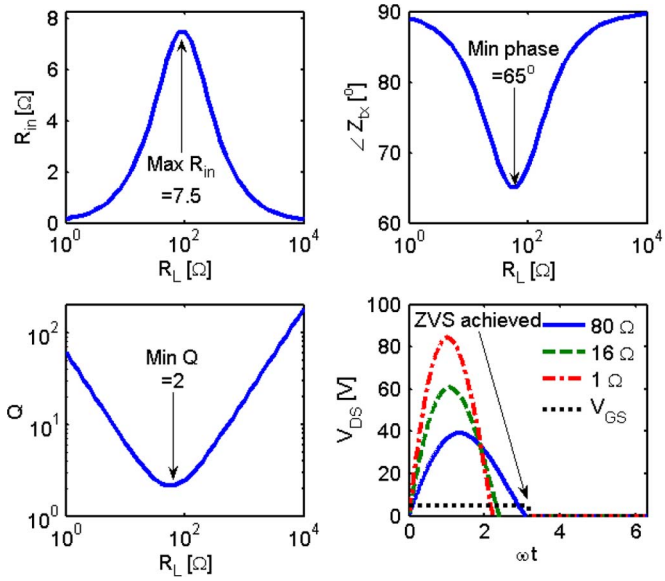

Fig. 4. From top left, clockwise: $R_{\rm in}$, $\angle Z_{\rm tx}$, drain voltage waveform at three R_L values, with a gate voltage for reference, and Q.

of the test system. Based on the proposed method and the equations in Section II, the optimum component values were calculated. Table I gives values of the inductances L_1, L_2, and M, which were measured at 240 kHz using an HP 4192A LF impedance analyzer, and the design parameters R_0, Q, and ϕ. Table II gives the calculated component values and lists the measured (at 240 kHz) values of the actual components being used, as well as their parasitic resistances. R_0 was chosen as 7.5 Ω based on the total component and coil parasitics, which amounted to 0.58 Ω. In general, selection of R_0 is system dependent, but it should be at least an order of magnitude higher than the parasitics, because the peak transmitting coil efficiency will be $R_0/(R_p + R_0)$ (where R_p is the parasitic on the transmitter side). In this case, R_0 of 7.5 Ω is about 13 times R_p, or an efficiency value of about 93%. A larger R_0 value will result in higher efficiency, but how large an R_0 value is acceptable depends on the availability of inductors of sufficient size to achieve minimum Q. Minimum Q and ϕ values were chosen based on allowable values given in [14] and [15], with an additional buffer to tolerate some deviations of real components. Fig. 4 shows the calculated $R_{\rm in}$, $\angle Z_{\rm tx}$,

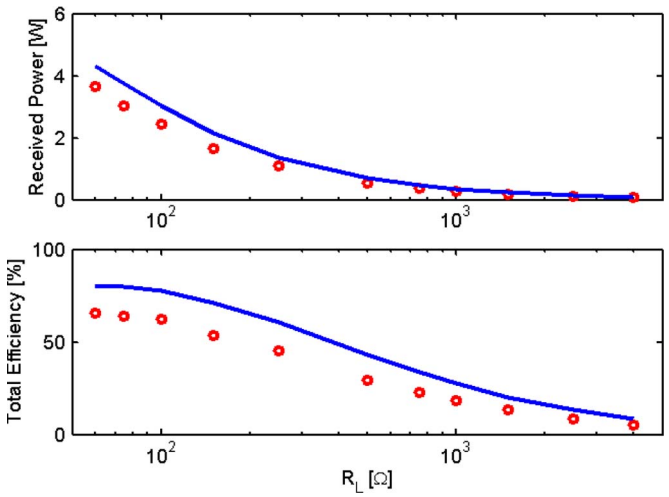

Fig. 5. Received power and total efficiency as a function of R_L. (Circles) Measured values. (Solid line) Simulated using the calculated component values.

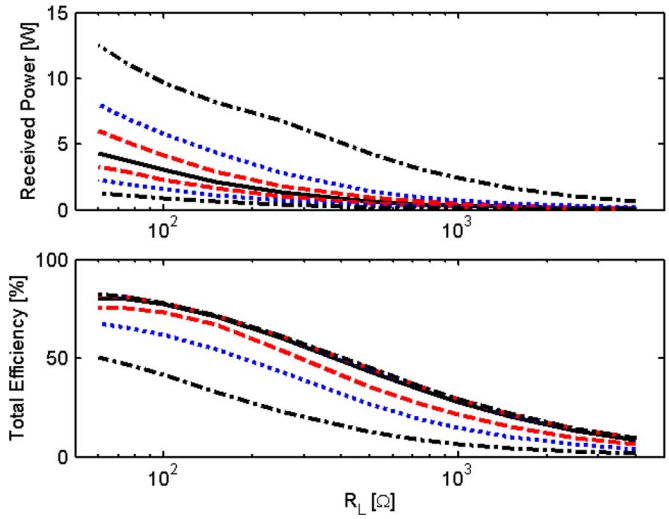

Fig. 6. Received power and total efficiency as a function of R_L, as well as their 95% confidence intervals with (red dashed line) 5% component tolerance, (blue dotted line) 10% component tolerance, and (black dash-dotted line) 20% component tolerance.

drain voltage waveform, and Q, demonstrating that the desired constraints are met using the component selection formulas.

One of the key challenges for a wireless power system is to have desirable performance responding to a variable load. To evaluate the system performance with regard to power and efficiency, R_L was swept from 60 to 4000 Ω by means of an electronic load. The dc voltage and current were measured at the load and at the supply. The transmitted power was measured using a current probe (Agilent N2783A), a voltage probe (Agilent N2863A), and an oscilloscope (Agilent DSO 5034A), whereas the received power was measured using the dc electronic load (BK 8500).

Fig. 5 shows the received power and total efficiency versus load resistance, as well as the simulated values of power and efficiency, using the ideal calculated component values. The system has power delivery of over 3.7 W and peak efficiency of over 66%. The important feature in Fig. 5 is the trend of decreasing received power and total efficiency with increasing R_L, which is guaranteed by component selection. This trend is what allows the system to charge a battery and be open loop, contrasted with closed-loop wireless power systems such as [9]. A charging battery looks like a resistance (represented by R_L), which increases with increasing charge. Thus, as the battery approaches full charge, the system would deliver less and less power. The ideal performance (solid line) is close to the real system (circles). Power and efficiency are lower by 5% to 10% in the actual system, primarily due to the deviation of L_{out} and C_{out} in the real components. Deviations from their ideal values cause ϕ and Q to shift, which has a substantial effect on the class-E efficiency.

To further investigate the sensitivity to component selection, a Monte Carlo simulation was run, assuming the components are normally distributed, with means given by the derived component formulas and with standard deviations σ, such that 3σ is the component tolerance. These simulations were carried out at component tolerance levels of 5%, 10%, and 20%. Fig. 6 shows the 95% confidence intervals for the received power and total efficiency at the three tolerance levels. As can be seen, the power is skewed low, with tolerances (in terms of upper

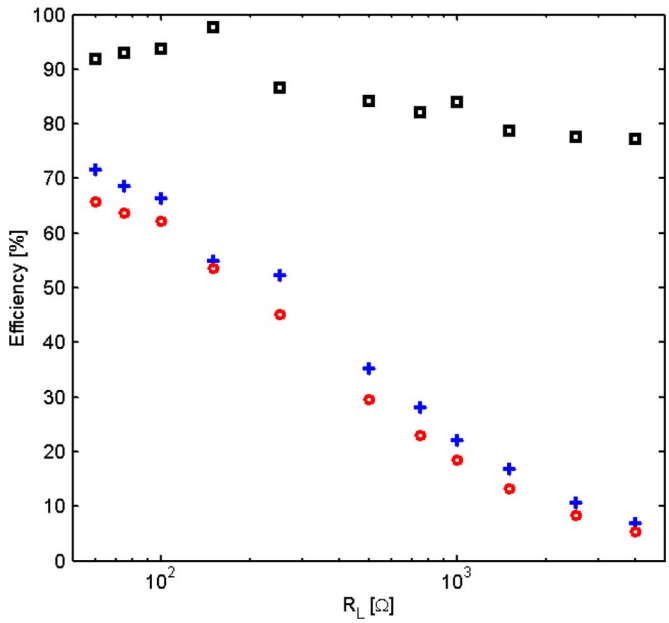

Fig. 7. Efficiency as a function of R_L. (Black squares) Class-E efficiency. (Blue pluses) Coupling efficiency. (Red circles) Total efficiency.

bound/lower bound, as a percentage difference from the mean) of about $+35/-25\%$ at 5% component tolerance, $+115/-45\%$ at 10% component tolerance, and $+425/-70\%$ at 20% component tolerance. The efficiency is skewed very high, with tolerances of about $+3.4/-18\%$ at 5% component tolerance, $+3.6/-38\%$ at 10% component tolerance, and $+4.3/-70\%$ at 20% component tolerance. This skew low in the power confidence intervals and skew high in the efficiency confidence intervals shows that the system is not optimized for maximum power delivery, but rather efficiency. This makes sense, as all of the constraints (R_0, ϕ, Q, and ZVS) used for component selection are chosen to maximize the efficiency of the class E. At a tolerance of 5% or less, the confidence interval shows

that the performance is still decent. For greater tolerances, the potential variability of performance is probably unacceptable for most applications.

Fig. 7 shows the amplifier efficiency, coupling efficiency, and total efficiency. The amplifier efficiency is ac transmitting power over dc input power; the coupling efficiency is dc power at the load over ac transmitted power, and the total efficiency is the product of these two efficiency values. In Fig. 7, the coupling efficiency comprises most of the losses. The coupling efficiency decreases with increasing load resistance, because as R_L increases, $R_{\rm in}$ decreases, whereas the parasitics remain the same; thus, more power is dissipated through the parasitics, the dominant losses being in the transmitting coil and in $L_{\rm out}$. Thus, while component selection is performed to optimize the amplifier efficiency, it does nothing for the coupling efficiency. The coupling efficiency could be improved by mitigating parasitics or increasing the mutual inductance. The amplifier efficiency peaks where $\angle Z_{\rm tx}$ is in the 40°–70° range, which by design is in the neighborhood of the phase minimum.

IV. Conclusion

This brief has presented a set of design equations for optimizing the performance of a class-E amplifier used in an inductively coupled wireless power system. By applying constraints on the real part of the input impedance to the primary coil, the phase of the input impedance, the minimum Q, and the drain voltage waveform, components can be selected to guarantee desirable operating characteristics of the system, namely, the ZVS operation of the class E and the trend of decreasing power received with increasing load resistance. The proposed optimization method was tested in a system composed of a 16 cm $\times$ 18 cm primary coil and a 4 cm $\times$ 5 cm secondary coil with a variable load. The system shows power delivery of over 3.7 W and peak efficiency of over 66%, in addition to the desirable trend of decreasing power and efficiency with respect to increasing load resistance.

References

[1] L. Collins, "Cutting the cord," *Eng. Technol.*, vol. 2, no. 6, pp. 30–33, Jun. 2007.

[2] W. Brown, "The history of power transmission by radio waves," *IEEE Trans. Microw. Theory Tech.*, vol. MTT-32, no. 9, pp. 1230–1242, Sep. 1984.

[3] G. Joung and B. Cho, "An energy transmission system for an artificial heart using leakage inductance compensation of transcutaneous transformer," *IEEE Trans. Power Electron.*, vol. 13, no. 6, pp. 1013–1022, Nov. 1998.

[4] Y. Jang and M. Jovanovic, "A contactless electrical energy transmission system for portable-telephone battery chargers," *IEEE Trans. Ind. Electron.*, vol. 50, no. 3, pp. 520–527, Jun. 2003.

[5] G. Wang, W. Liu, R. Bashirullah, M. Sivaprakasam, G. Kendir, Y. Ji, M. Humayun, and J. Weiland, "A closed loop transcutaneous power transfer system for implantable devices with enhanced stability," in *Proc. ISCAS*, 2004, vol. 4, pp. 17–20.

[6] J. Acero, D. Navarro, L. Barragan, I. Garde, J. Artigas, and J. Burdio, "FPGA-based power measuring for induction heating appliances using sigma–delta A/D conversion," *IEEE Trans. Ind. Electron.*, vol. 54, no. 4, pp. 1843–1852, Aug. 2007.

[7] N. Sokal and A. Sokal, "Class E—A new class of high-efficiency tuned single-ended switching power amplifiers," *IEEE J. Solid-State Circuits*, vol. SSC-10, no. 3, pp. 168–176, Jun. 1975.

[8] C. Wang, G. Covic, and O. Stielau, "Power transfer capability and bifurcation phenomena of loosely coupled inductive power transfer systems," *IEEE Trans. Ind. Electron.*, vol. 51, no. 1, pp. 148–157, Feb. 2004.

[9] G. Kendir, W. Liu, G. Wang, M. Sivaprakasam, R. Bashirullah, M. Humayun, and J. Weiland, "An optimal design methodology for inductive power link with class-E amplifier," *IEEE Trans. Circuits Syst. I, Reg. Papers*, vol. 52, no. 5, pp. 857–866, May 2005.

[10] H. Sekiya, I. Sasase, and S. Mori, "Computation of design values for class E amplifiers without using waveform equations," *IEEE Trans. Circuits Syst. I, Fundam. Theory Appl.*, vol. 49, no. 7, pp. 966–978, Jul. 2002.

[11] Z. N. Low, R. A. Chinga, R. Tseng, and J. Lin, "Design and test of a high-power high-efficiency loosely coupled planar wireless power transfer system," *IEEE Trans. Ind. Electron.*, vol. 56, no. 5, pp. 1801–1812, May 2009.

[12] J. J. Casanova, Z. N. Low, and J. Lin, "A loosely coupled planar wireless power system for multiple receivers," *IEEE Trans. Ind. Electron.*, vol. 56, no. 8, pp. 3060–3068, Aug. 2009.

[13] F. Raab, "Idealized operation of the class E tuned power amplifier," *IEEE Trans. Circuits Syst.*, vol. CAS-24, no. 12, pp. 725–735, Dec. 1977.

[14] N. Sokal, "Class-E RF power amplifiers," *QEX*, vol. 204, pp. 9–20, 2001.

[15] F. Raab, "Effects of circuit variations on the class E tuned power amplifier," *IEEE J. Solid-State Circuits*, vol. SSC-13, no. 2, pp. 239–247, Apr. 1978.

[16] J. J. Casanova, Z. N. Low, J. Lin, and R. Tseng, "Transmitting coil achieving uniform magnetic field distribution for planar wireless power transfer system," in *Proc. Radio Wireless Symp.*, 2009, pp. 530–533.